Ma *et al. Complex Eng Syst* 2023;3:10
DOI: 10.20517/ces.2023.14

Complex Engineering Systems

Research Article

Open Access

Fixed-time integral sliding mode tracking control of a wheeled mobile robot

Ling Ma, Chenghu Wang, Cheng Ge, Hui Liu, Bo Li

Institute of Logistics Science and Engineering, Shanghai Maritime University, Shanghai 201306, China.

Correspondence to: Associate Prof. Bo Li, Institute of Logistics Science and Engineering, Shanghai Maritime University, Shanghai 201306, China. E-mail: libo@shmtu.edu.cn

How to cite this article: Ma L, Wang C, Ge C, Liu H, Li B. Fixed-time integral sliding mode tracking control of a wheeled mobile robot. *Complex Eng Syst* 2023;3:10. http://dx.doi.org/10.20517/ces.2023.14

Received: 1 May 2023 **First Decision:** 29 May 2023 **Revised:** 13 Jun 2023 **Accepted:** 20 Jun 2023 **Published:** 29 Jun 2023

Academic Editor: Mouquan Shen **Copy Editor:** Yanbing Bai **Production Editor:** Yanbing Bai

Abstract

This paper presents a fixed-time integral sliding mode control scheme for a nonholonomic wheeled mobile robot (WMR). To achieve the trajectory tracking mission, the dynamic model of a WMR is first transformed into a second-order attitude subsystem and a third-order position subsystem. Two novel continuous fixed-time disturbance observers are proposed to estimate the external disturbances of the two subsystems, respectively. Then, trajectory tracking controllers are designed for two subsystems by utilizing the reconstructed information obtained from the disturbance observers. Additionally, an auxiliary variable that incorporates the Gaussian error function is introduced to address the chattering problem of the control system. Finally, the proposed control scheme is validated by a wheeled mobile robotic experimental platform.

Keywords: Wheeled mobile robot, trajectory tracking, disturbance observer, fixed-time stability, integral sliding mode control

1. INTRODUCTION

During the past decades, the wheeled mobile robot (WMR) has attracted extensive attention as it is widely used in various fields. The research on the WMR mainly includes robot positioning, motion planning, and motion control, among which the motion control is a fundamental problem. There are three main parts of the motion control, including point stabilization, path planning, and trajectory tracking[1]. The trajectory

tracking control is a significant field in motion control, which has been studied extensively in recent years[2]. In practical engineering applications, a WMR is a highly coupled system with nonholonomic constraints and external disturbances. Hence, it is significant to design an anti-interference trajectory tracking control scheme with superior performance. At present, the design of the tracking controller of a WMR is mainly based on two types: one is to consider only the kinematic model[3], while the other is to design on the basis of kinematic and dynamic models[4]. The kinematic model-based control only considers the linear velocity and angular velocity as the control inputs. Compared with the kinematic model, the introduction of dynamic models can solve the external disturbance problem and the crucial nonholonomic constraint problem[5].

In[6], the system with nonhonolomic constraints was transformed into an extended chain system by coordinate transformation. On this basis, some scholars have designed the trajectory tracking control schemes by transforming the kinematic model of a WMR into a chain structure[7]. In practice, there is a problem called "excellent velocity tracking"[8] when designing a trajectory tracking controller only based on a kinematic system. Thus, it is more reasonable to take the force or torque as inputs of the control system instead of the speed. Meanwhile, external disturbances can be further taken into account. Nevertheless, the design process of the controller that simultaneously incorporates both the kinematic and dynamic models is complicated. The work of Zhai and Song[9] transformed the dynamic error system into second-order and third-order subsystems. And an intermediate variable related to the position error is introduced to tackle the problem of constructing a control method for a third-order system using the terminal sliding mode control. However, the aforementioned control schemes can only achieve finite time stability. It is noteworthy that the upper limit of the convergence time is unknown and dependent on the initial states of the control system. To overcome this problem, fixed-time stable control methods are proposed[10]. In reference[11], a new integral sliding mode-based control (ISMC) scheme was developed and applied on the dynamic model of the WMR to enable the WMR to track the desired trajectory in a fixed time. However, there exists the singularity problem, making the WMR unable to track the arbitrary trajectories and limiting its practical application when the desired angular velocity is zero.

In the practical motion environment, there are external disturbances and uncertainties that can deteriorate the performance of the control system. To cope with the problem, an observer-based control scheme is an efficient method with disturbance-rejection performance[12]. The traditional observers can only achieve asymptotic stability of the observation errors, whereas the finite time disturbance observers were designed to improve the performance of the observer[13]. On this basis, the fault-tolerant attitude control problem of spacecraft under external disturbances was solved by the introduction of a continuous finite-time observer[14], which also restrains the chattering phenomenon. Zhang *et al.* put forward a novel continuous practical fixed-time disturbance observer and applied it on a WMR, which can not only avoid the chattering problem but also improve the ability to attenuate disturbance[15]. Different from the work of Zhang, the Gaussian error function, which is sometimes called probability integral[16], can also be used to develop a control scheme that improves the chattering problem[17].

Motivated by the above discussions, an integral sliding mode-based fixed-time trajectory tracking control scheme is proposed by combining the kinematic model with the dynamic model of a WMR in this paper. **(1)** A continuous fixed-time disturbance observer using the Gaussian error function is proposed, which avoids the chattering problem and estimates the external disturbance of a WMR accurately. **(2)** An auxiliary variable incorporating variable exponential coefficients is introduced to simplify the design process of the controller for the third-order subsystem and avoid the singularity problem simultaneously. **(3)** The reliability and effectiveness of the designed control scheme are verified by a comparative experiment conducted on a wheeled mobile experimental platform.

2. PRELIMINARIES AND PROBLEM STATEMENT

2.1. Preliminaries

Lemma 1 [18] *Consider the following system as*

$$\dot{\boldsymbol{x}} = f(\boldsymbol{x}),\ \boldsymbol{x}(0) = \boldsymbol{x_0},\ \boldsymbol{x} \in R \tag{1}$$

If there exists a positive definite Lyapunov function $V(\boldsymbol{x})$*, which satisfies* $\dot{V}(\boldsymbol{x}) \leq -m_1 V^a(\boldsymbol{x}) - n_1 V^b(\boldsymbol{x}) + \varrho$*, where* m_1, n_1*, and* ϱ *are all positive constants.* $0 < a < 1, b > 1$ *are real numbers. Then the origin of the system (2) is fixed-time stable, and the settling time is bounded by* $t_1 \leq \frac{1}{m_1\vartheta(1-a)} + \frac{1}{n_1\vartheta(b-1)}$ *with* $0 < \vartheta < 1$.

Lemma 2 [16] *The Gaussian error function is defined as follows:*

$$\operatorname{erf}(x) = \frac{2}{\sqrt{\pi}} \int_0^x e^{-2t^2} \mathrm{dt} \tag{2}$$

where e is the natural constant. If $0 \leq x < 1$*, then the Gaussian error function will satisfy* $\frac{1}{2}x \leq \operatorname{erf}(x) \leq 2x$.

Lemma 3 [19] *For* $x \in \mathbf{R}$ *and* $\mu > 0$*, one gets the following chain of inequalities:* $x\tanh(\frac{x}{\mu}) < x\operatorname{erf}(\frac{x}{\mu}) < |x|$.

Lemma 4 [20] *The following inequality will hold* $|x| - \frac{\varepsilon}{\kappa} \leq x\tanh(\kappa x)$ *for any* $\kappa > 0$ *and for any* $\varepsilon \in \mathbf{R}$*, where* $\varepsilon = e^{-(\varepsilon+1)}$*. Then,* $\varepsilon = 0.2785$ *can be obtained.*

2.2. Dynamic model of WMR

A nonholonomic WMR system is shown in Figure 1. It consists of two balance wheels and two driving wheels, and the line between the balance wheels is perpendicular to the line between the driving wheels. The distance between the driving wheel and the barycentric coordinate is R, and r is the radius of the driving wheel. The position and attitude control is achieved by independent direct current motors, which provide the appropriate torques to the driving wheels. One assumes that the center of mass of the WMR coincides with the geometric center. Then, the dynamic model of the WMR is expressed in the form of[21]

$$\begin{cases} \dot{x} = v\cos\theta \\ \dot{y} = v\sin\theta \\ \dot{\theta} = \omega \\ J\dot{\omega} = u_1 + d_1 \\ m\dot{v} = u_2 + d_2 \end{cases} \tag{3}$$

with $u_1 = \frac{R}{r}(\tau_1 - \tau_2)$, and $u_2 = \frac{1}{r}(\tau_1 + \tau_2)$. τ_1 and τ_2 present the control torques. v and ω are the linear and angular velocities of the WMR, respectively. m denotes the mass, and J the moment of inertia. (x, y) is the actual coordinates. θ is the orientation of the vehicle counterclockwise from the positive direction of the X axis. $(\dot{x}, \dot{y}, \dot{\theta})$ denotes the motion of the WMR. d_1 and d_2 represent the external disturbances.

The reference trajectory is defined as

$$\begin{cases} \dot{x}_r = v_r\cos\theta_r \\ \dot{y}_r = v_r\sin\theta_r \\ \dot{\theta}_r = \omega_r \end{cases} \tag{4}$$

where x_r, y_r, and θ_r denote the position and attitude states of the virtual WMR, respectively.

Assumption 1: Suppose ω_r, $\dot{\omega}_r$, v_r, and $\dot{v}_r$ are satisfied with $|\omega_r| \leq \omega_{r_{\max}}$, $|\dot{\omega}_r| \leq \omega_{1_{\max}}$, $|v_r| \leq v_{r_{\max}}$, And $|\dot{v}_r| \leq v_{1_{\max}}$, where $\omega_{r_{\max}}$, $\omega_{1_{\max}}$, $v_{r_{\max}}$, and $v_{1_{\max}}$ are positive constants.

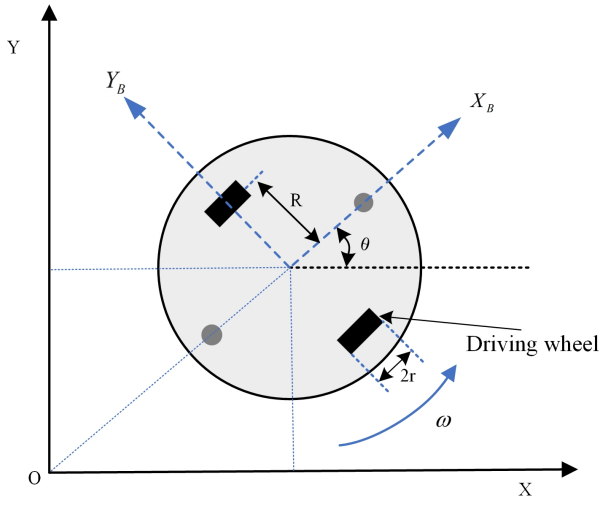

Figure 1. Physical model of a WMR. WMR: wheeled mobile robot.

Assumption 2: Suppose the d_1, d_2, and their derivatives exist with bounds, which is given by $|d_1| \leq k_{1m}$, $|d_2| \leq k_{2m}$, where k_{1m} and k_{2m} are all positive constants.

Then, the tracking errors of the WMR are expressed as

$$\begin{bmatrix} x_e \\ y_e \\ \theta_e \end{bmatrix} = \begin{bmatrix} \cos\theta & \sin\theta & 0 \\ -\sin\theta & \cos\theta & 0 \\ 0 & 0 & 1 \end{bmatrix} \begin{bmatrix} x - x_r \\ y - y_r \\ \theta - \theta_r \end{bmatrix}. \tag{5}$$

Furthermore, the error dynamics system could be transformed in the form of

$$\begin{cases} \dot{x}_e = \omega y_e - v + v_r \cos\theta_e \\ \dot{y}_e = v_r \sin\theta_e - \omega x_e \\ \dot{\theta}_e = \omega - \omega_r \\ J\dot{\omega} = u_1 + d_1 \\ m\dot{v} = u_2 + d_2 \end{cases} \tag{6}$$

To simplify the whole design process, the system (6) can be divided into two subsystems, which contain a second-order subsystem:

$$\begin{cases} \dot{\theta}_e = \omega - \omega_r \\ J\dot{\omega} = u_1 + d_1 \end{cases} \tag{7}$$

and a third-order subsystem:

$$\begin{cases} \dot{x}_e = \omega y_e - v + v_r \cos\theta_e \\ \dot{y}_e = v_r \sin\theta_e - \omega x_e \\ m\dot{v} = u_2 + d_2 \end{cases} \tag{8}$$

3. FIXED-TIME TRAJECTORY CONTROL

In this section, a fixed-time sliding mode control scheme is developed to realize the fast and high-accuracy trajectory tracking control of a WMR under external disturbances. Firstly, a fixed-time disturbance observer

and a new fixed-time sliding mode surface are proposed for the second-order subsystem (7). On this basis, a fixed-time controller is constructed to make the error variables, θ_e and $\dot{\theta}_e$, converge into a small region around the origin. Then, a fixed-time controller is developed for the third-order subsystem (8), which guarantees that the system state variables, x_e, y_e, and v, are all uniformly ultimately bounded, and the tracking errors, x_e and y_e, can converge into a small region around the origin in a fixed time.

3.1. Tracking control laws design for the second-order subsystem

3.1.1. Fixed-time disturbance observer

Firstly, for the attitude error subsystem (7), define an auxiliary variable as

$$\varsigma_1 = \omega - \varpi_1 \tag{9}$$

where ϖ_1 satisfies

$$\dot{\varpi}_1 = \frac{1}{J}u_1 + l_{11}\,\mathrm{erf}(\varsigma_1) + l_{12}|\varsigma_1|^{\gamma_1}\,\mathrm{erf}(\varsigma_1) \tag{10}$$

The parameters l_{11} and l_{12} are positive constants with $l_{11} > k_{1m}/J$. Let variable exponential coefficient $\gamma_1 = \frac{\lambda_0\varsigma_1^2}{1+\mu_0\varsigma_1^2}$ with λ_0 and μ_0 satisfying $0 < \mu_0 < 1$ and $1 + \mu_0 < \lambda_0$.

Theorem 1 *For the second-order subsystem (7), if the disturbance observer is constructed as*

$$\hat{d}_1 = J\Big(l_{11}\,\mathrm{erf}(\varsigma_1) + l_{12}|\varsigma_1|^{\gamma_1}\,\mathrm{erf}(\varsigma_1)\Big) \tag{11}$$

then it can estimate d_1 accurately in a fixed time. That is to say, the observation error $\tilde{d}_1 = d_1 - \hat{d}_1$ can converge into a small region within a fixed time.

Proof of Theorem 1 Select a Lyapunov function as $V_2 = \varsigma_1^2$, differentiating it, one has

$$\begin{aligned}
\dot{V}_2 &= 2\varsigma_1(\dot{\omega} - \dot{\varpi}_1)\\
&= 2\varsigma_1\Big(\frac{1}{J}(u_1 + d_1) - \big(\frac{1}{J}u_1 + l_{11}\,\mathrm{erf}(\varsigma_1) + l_{12}|\varsigma_1|^{\gamma_1}\,\mathrm{erf}(\varsigma_1)\big)\Big)\\
&= 2\varsigma_1\Big(-l_{11}\,\mathrm{erf}(\varsigma_1) - l_{12}|\varsigma_1|^{\gamma_1}\,\mathrm{erf}(\varsigma_1) + \frac{1}{J}d_1\Big)\\
&= -2\Big(l_{11}\varsigma_1\,\mathrm{erf}(\varsigma_1) - \frac{1}{J}\varsigma_1 d_1 + l_{12}\varsigma_1|\varsigma_1|^{\gamma_1}\,\mathrm{erf}(\varsigma_1)\Big)\\
&\le -2\Big(l_{11}\varsigma_1\tanh(\varsigma_1) - \frac{1}{J}\varsigma_1 d_1 + l_{12}\varsigma_1|\varsigma_1|^{\gamma_1}\,\mathrm{erf}(\varsigma_1)\Big)\\
&\le -2\Big(l_{11}|\varsigma_1| - l_{11}\epsilon_1 - \frac{k_{1m}}{J}|\varsigma_1| + l_{12}\varsigma_1|\varsigma_1|^{\gamma_1}\,\mathrm{erf}(\varsigma_1)\Big)\\
&\le -2l_{12}|\varsigma_1||\varsigma_1|^{\gamma_1}\,\mathrm{erf}(|\varsigma_1|) + 2l_{11}\epsilon_1\\
&= -2l_{12}|\varsigma_1|^{\gamma_1+1}\,\mathrm{erf}(|\varsigma_1|) + 2l_{11}\epsilon_1
\end{aligned} \tag{12}$$

where ϵ_1 is a positive constant.

Case 1 When $V_2 > 1$ and $|\varsigma_1| > 1$, one has $\mathrm{erf}(|\varsigma_1|) > \mathrm{erf}(1)$ and $\frac{\lambda_0\varsigma_1^2}{1+\mu_0\varsigma_1^2} \ge \frac{\lambda_0}{1+\mu_0} > 1$. Then (12) can be rewritten as

$$\begin{aligned}
\dot{V}_2 &\le -2(l_{12}\,\mathrm{erf}(1) - l_{11}\epsilon_1)|\varsigma_1|^{\frac{\lambda_0}{1+\mu_0}+1}\\
&\le -2(l_{12}\,\mathrm{erf}(1) - l_{11}\epsilon_1)V_2^{\frac{\lambda_0+\mu_0+1}{2(1+\mu_0)}}
\end{aligned} \tag{13}$$

As $l_{12}\,\mathrm{erf}(1) - l_{11}\epsilon_1 > 0$ and $\bar{\gamma}_1 = \frac{\lambda_0+\mu_0+1}{2(1+\mu_0)} > 1$, then all the solutions of $\{V_2 > 1\}$ will reach the set $\{V_2 \le 1\}$ within a fixed time $t_{f1} \le \frac{1}{2(l_{12}\,\mathrm{erf}(1)-l_{11}\epsilon_1)(\bar{\gamma}_1-1)}$.

Case 2 In the converse case $V_2 \leq 1$, one has

$$\dot{V}_2 \leq -2l_{12}|\varsigma_1||\varsigma_1|^{\gamma_1}\operatorname{erf}(|\varsigma_1|) + 2l_{11}\epsilon_1 \tag{14}$$

As $1+\mu_0\varsigma_1^2 \geq 1$ and $|\varsigma_1| \leq 1$, it can be obtained that $\min\left(|\varsigma_1|^{\gamma_1}\right) \geq \min\left(|\varsigma_1|^{\lambda_0\varsigma_1^2}\right) = e^{\frac{-\lambda_0}{2e}}$. Considering the Lemma 3, then (14) is converted into the following form

$$\begin{aligned}
\dot{V}_2 &\leq -2l_{12}|\varsigma_1||\varsigma_1|^{\gamma_1}\tanh(|\varsigma_1|) + 2l_{11}\epsilon_1 \\
&\leq 2l_{12}|\varsigma_1||\varsigma_1|^{\gamma_1} + 2l_{12}|\varsigma_1|^{\gamma_1}\epsilon_2 + 2l_{11}\epsilon_1 \\
&\leq -2l_{12}|\varsigma_1||\varsigma_1|^{\gamma_1} + 2l_{12}\epsilon_2 + 2l_{11}\epsilon_1 \\
&\leq -2l_{12}|\varsigma_1|^{\gamma_1+1} + 2l_{11}\epsilon_1 + 2l_{12}\epsilon_2 \\
&\leq -2l_{12}e^{\frac{-\lambda_0}{2e}}|\varsigma_1| + 2l_{11}\epsilon_1 + l_{12}\epsilon_2 \\
&\leq -b_1V_2^{\frac{1}{2}} + \tilde{\epsilon} \\
&\leq -l_{13}b_1V_2^{\frac{1}{2}} - (1-l_{13})b_1V_2^{\frac{1}{2}} + \tilde{\epsilon}
\end{aligned} \tag{15}$$

with $b_1 = 2l_{12}e^{\frac{-\lambda_0}{2e}}$, and $\tilde{\epsilon} = 2l_{11}\epsilon_1 + 2l_{12}\epsilon_2$. When $0 < l_{13} < 1$, and $\tilde{\epsilon} - (1-l_{13})b_1V_2^{\frac{1}{2}} \geq 0$, (15) can be simplified as $\dot{V}_2 \leq -l_{13}b_1V_2^{\frac{1}{2}}$. Then, the solution of V_2 will reach a small set Δ_1, which is defined as $\Delta_1 = \left\{\varsigma_1 | V_1(\varsigma_1) \leq (\frac{\tilde{\epsilon}}{b_1(1-l_{13})})^2\right\}$ within a settling time $t_{f2} \leq \frac{2}{b_1 l_{13}}$.

In view of the above two cases, the auxiliary variable ς_1 will converge into a small set $\Delta_1 = \left\{\varsigma_1 | V_1(\varsigma_1) \leq (\frac{\tilde{\epsilon}}{b_1(1-l_{13})})^2\right\}$ within settling time $t_f = t_{f1} + t_{f2}$.

Then, the disturbance observation error

$$\begin{aligned}
\tilde{d}_1 &= d_1 - \hat{d}_1 \\
&= d_1 - J\left(l_{11}\operatorname{erf}(\varsigma_1) + l_{12}|\varsigma_1|^{\gamma_1}\operatorname{erf}(\varsigma_1)\right)
\end{aligned} \tag{16}$$

The disturbance d_1 is bounded according to Assumption 1. Thus, the disturbance observer (11) can estimate d_1 accurately, and the observation error $\tilde{d}_1$ can remain in a small set $\Delta_2 = \left\{\varsigma_1 \middle| |\varsigma_1| \leq k_{1m} + J\left(l_{11}\operatorname{erf}(\Delta_1) + l_{12}|\Delta_1|^{\bar{\gamma}_1}\operatorname{erf}(\Delta_1)\right)\right\}$ after a fixed time, where $\bar{\gamma}_1 = \frac{\lambda_0\Delta_1^2}{1+\mu_0\Delta_1^2}$.

3.1.2. Fixed-time sliding mode controller

For the subsystem (7), define $\omega_e = \omega - \omega_r$. A fixed-time integral sliding mode surface is introduced as follows[22]

$$s_1 = \omega_e + \int_0^t \left(k_{11}(\lceil\theta_e\rfloor^{p_1} + \lceil\theta_e\rfloor^{q_1}) + k_{12}(\lceil\omega_e\rfloor^{p_2} + \lceil\omega_e\rfloor^{q_2})\right)\mathrm{d}\tau \tag{17}$$

with $0 < p_i < 1$, $q_i > 1$, and $(i = 1, 2)$. For any $x \in \mathrm{R}$, $\alpha \in \mathrm{R}^+$, the notation is defined as $\lceil x\rfloor^\alpha = |x|^\alpha \operatorname{sign}(x)$. Based on the sliding mode surface as (17), the fixed-time controller is designed as follows:

$$u_1 = -J\left(k_{11}(\lceil\theta_e\rfloor^{p_1} + \lceil\theta_e\rfloor^{q_1}) + k_{12}(\lceil\omega_e\rfloor^{p_2} + \lceil\omega_e\rfloor^{q_2}) + \alpha_1\lceil s_1\rfloor^{p_3} + \alpha_2\lceil s_1\rfloor^{q_3} + \alpha_3\operatorname{erf}(s_1) - \dot{\omega}_r\right) - \hat{d}_1 \tag{18}$$

where $\alpha_i, k_{1i}, (i = 1, 2)$ are positive constants, α_3 satisfies $\alpha_3 \geq \frac{k_{1m}}{J}$. In addition, $p_i, q_i, (i = 1, 2, 3)$ are all positive odd integers with $0 < p_i < 1, q_i > 1$.

Theorem 2 *For the second-order system (7), if the fixed-time controller is constructed in the form of (18), then the real sliding mode variable will converge into a small set within a fixed time.*

Proof of Theorem 2 Choose a Lyapunov function as $V_3 = \frac{1}{2}s_1^2$ and refer to Lemma 2 to Lemma 4, the time derivative of V_3 is

$$\begin{aligned}\dot{V}_3 &= s_1\Big(\dot{\omega}_e + k_{11}(\lceil\theta_e\rfloor^{p_1} + \lceil\theta_e\rfloor^{q_1}) + k_{12}(\lceil\omega_e\rfloor^{p_2} + \lceil\omega_e\rfloor^{q_2})\Big)\\ &= s_1\Big(\frac{1}{J}(u_1 + d_1) - \dot{\omega}_r + k_{11}(\lceil\theta_e\rfloor^{p_1} + \lceil\theta_e\rfloor^{q_1}) + k_{12}(\lceil\omega_e\rfloor^{p_2} + \lceil\omega_e\rfloor^{q_2})\Big)\\ &= s_1\Big(-\alpha_1\lceil s_1\rfloor^{p_3} - \alpha_2\lceil s_1\rfloor^{q_3} - \alpha_3\,\mathrm{erf}(s_1) + \frac{1}{J}\tilde{d}_1\Big)\\ &\le -\alpha_1|s_1|^{p_3+1} - \alpha_2|s_1|^{q_3+1} - \alpha_3 s_1\tanh(s_1) + \frac{1}{J}|s_1||\tilde{d}_1|\\ &\le -2^{\bar{p}_3}\alpha_1 V_2^{\bar{p}_3} - 2^{\bar{q}_3}\alpha_2 V_2^{\bar{q}_3} + \bar{\vartheta}_1\end{aligned} \tag{19}$$

where $\bar{p}_3 = \frac{p_3+1}{2}, \bar{q}_3 = \frac{q_3+1}{2}, \bar{\vartheta}_1 = \alpha_3\vartheta_1$ with ϑ_1 being a positive constant. By using Lemma 4, the second-order system (7) is fixed-time stable. The sliding mode surface s_1 will converge into a small region $\Delta_3 = \Big\{s_1|V(s_1) \le \min\Big\{\big(\frac{c_2}{\alpha_1 2^{\bar{p}_3}}\big)^{\frac{1}{\bar{p}_3}}, \big(\frac{c_2}{\alpha_2 2^{\bar{q}_3}}\big)^{\frac{1}{\bar{p}_3}}\Big\}\Big\}$ around the origin in a fixed time t_{s_1}, which is determined by $t_{s_1} \le \frac{1}{\alpha_1 2^{\bar{p}_3}\phi_1(1-\bar{p}_3)} + \frac{1}{\alpha_2 2^{\bar{q}_3}\phi_1(\bar{q}_3-1)}$. Then, one can obtain that variables θ_e and ω_e converge to zero along the real sliding mode in a fixed time[23].

3.2. Tracking control laws design for the third-order subsystem

After the angular error θ_e converges to zero according to Theorem 2, one can obtain that $\sin\theta_e$ equals zero, and $\cos\theta_e$ equals 1. The system (8) can be simplified as

$$\begin{cases}\dot{x}_e = \omega_r y_e - v + v_r\\ \dot{y}_e = -\omega_r x_e\\ m\dot{v} = u_2 + d_2\end{cases} \tag{20}$$

3.2.1. Fixed-time disturbance observer

Introduce the following auxiliary variable for the simplified third-order subsystem (20)

$$\varsigma_2 = v - \varpi_2 \tag{21}$$

where ϖ_2 satisfies

$$\dot{\varpi}_2 = \frac{1}{m}u_2 + l_{21}\mathrm{erf}(\varsigma_2) + l_{22}|\varsigma_2|^{\gamma_2}\,\mathrm{erf}(\varsigma_2) \tag{22}$$

where $\gamma_2 = \frac{\lambda_3\varsigma_1^2}{1+\mu_3\varsigma_1^2}$, and λ_3 and μ_3 are integers satisfying the constraints: $0 < \mu_3 < 1$, $1 + \mu_3 < \lambda_3$. The parameters l_{21} and l_{22} are positive constants with $l_{21} > k_{2m}$ and $l_{22} > 0$.

Theorem 3 *For the simplified third-order subsystem (20), a fixed-time disturbance observer is developed in the form of*

$$\hat{d}_2 = m\Big(l_{21}\,\mathrm{erf}(\varsigma_2) + l_{22}|\varsigma_2|^{\gamma_2}\,\mathrm{erf}(\varsigma_2)\Big) \tag{23}$$

then it can estimate d_2 in a fixed time, and the observation error $\tilde{d}_2 = d_2 - \hat{d}_2$ can converge into a small region around the origin within a fixed time t_{d_2}.

Proof of Theorem 3 Similar to the proof of Theorem 1.

3.2.2. Fixed-time sliding mode controller

For the third-order subsystem (20), introduce the following auxiliary variable:

$$\xi = x_e + \int_0^t \Big(\lambda_1\,\mathrm{erf}(x_e) - \lambda_2\,\mathrm{erf}(y_e) + \lambda_3 x_e y_e\,\mathrm{erf}(y_e) + k_1|x_e|^{\gamma_3}\,\mathrm{erf}\big(\frac{x_e}{\epsilon_3}\big)\Big)\mathrm{d}\tau \tag{24}$$

where λ_1 λ_2, k_1, and ϵ_3 are positive constants, $\lambda_2 \leq \lambda_1 \operatorname{erf}(1)$. Let $\gamma_3 = \frac{\lambda_4 x_e^{\,2}}{1+\mu_4 x_e^{\,2}}$, with λ_4 and μ_4 being integers and $0 < \mu_4 < 1$, $1 + \mu_4 < \lambda_4$.

Select a fixed-time sliding mode surface as:

$$s_2 = \dot{\xi} + \int_0^t \left(k_{21} \left(\lceil \xi \rfloor^{p_4} + \lceil \xi \rfloor^{q_4} \right) + k_{22} \left(\lceil \dot{\xi} \rfloor^{p_5} + \lceil \dot{\xi} \rfloor^{q_5} \right) \right) \mathrm{d}\tau \tag{25}$$

where k_{21} and k_{22} are positive constants, $0 < p_i < 1$ and $q_i > 1$, $i = 4, 5$ are positive odd integers.

Theorem 4 *For the third-order subsystem (20), if the fixed-time sliding mode surface is chosen as (25) and the fixed-time controller is designed as (26),*

$$\begin{aligned} u_2 =& m \Big(\dot{v}_r + \dot{\omega}_r y_e + \omega_r \dot{y}_e + \dot{h}(x_e, y_e) + k_{21} \left(\lceil \xi \rfloor^{p_4} + \lceil \xi \rfloor^{q_4} \right) \\ &+ k_{22} \left(\lceil \dot{\xi} \rfloor^{p_5} + \lceil \dot{\xi} \rfloor^{q_5} \right) + \beta_1 \lceil s_2 \rfloor^{p_6} + \beta_2 \lceil s_2 \rfloor^{q_6} + \beta_3 \operatorname{erf}(s_2) \Big) + \hat{d}_2 \end{aligned} \tag{26}$$

then the sliding mode surface s_2 is fixed-time stable, which will converge into a small region of origin within settling time $t_{s_2} \leq \frac{1}{\alpha_4 2^{\bar{p}_6} \phi_2 (1-\bar{p}_6)} + \frac{1}{\alpha_5 2^{\bar{q}_6} \phi_2 (\bar{q}_6 - 1)}$. $h(x_e, y_e) = \lambda_1 \operatorname{erf}(x_e) - \lambda_2 \operatorname{erf}(y_e) + \lambda_3 x_e y_e \operatorname{erf}(y_e) + k_1 |x_e|^{\gamma_3} \operatorname{erf}\left(\frac{x_e}{\epsilon_2}\right)$, in which β_1, β_2 are positive constants, and p_6, q_6 are positive odd integers satisfying $0 < p_6 < 1$, $q_6 > 1$.

Proof of Theorem 4 The proof process will be conducted in 3 steps: (1) After the angular error θ_e converges to zero according to Theorem 2, s_2 and the auxiliary variable ξ can converge into a small region around the origin within a fixed time; (2) The error variables x_e, y_e can converge into a small region around the origin within a fixed time; (3) It should be proved that x_e and y_e do not escape to infinity before the angular error θ_e converges to zero.

Step 1 Select a positive Lyapunov function $V_4 = \frac{1}{2} s_2^2$, differentiating it and substituting (24)-(26) yields to

$$\begin{aligned} \dot{V}_4 &= s_2 \dot{s}_2 \\ &= s_2 \Big(-\beta_1 \lceil s_2 \rfloor^{p_6} - \beta_2 \lceil s_2 \rfloor^{q_6} - \beta_3 \operatorname{erf}(s_2) + \frac{1}{m} (\hat{d}_2 - d_2) \Big) \\ &\leq -\beta_1 |s_2|^{p_6+1} - \beta_2 |s_2|^{q_6+1} - \beta_3 s_2 \operatorname{erf}(s_2) + \frac{1}{m} s_2 \tilde{d}_2 \\ &\leq -\beta_1 |s_2|^{p_6+1} - \beta_2 |s_2|^{q_6+1} - \beta_3 s_2 \tanh(s_2) + \frac{1}{m} s_2 \tilde{d}_2 \\ &\leq -\beta_1 |s_2|^{p_6+1} - \beta_2 |s_2|^{q_6+1} - \beta_3 |s_2| + \frac{1}{m} |s_2| |\tilde{d}_2| \\ &\leq -2^{\bar{p}_6} \beta_1 V_3^{\bar{p}_6} - 2^{\bar{q}_6} \beta_2 V_3^{\bar{q}_6} + \bar{\vartheta}_2 \end{aligned} \tag{27}$$

where $\bar{p}_6 = \frac{p_6+1}{2}$, $\bar{q}_6 = \frac{q_6+1}{2}$, $\bar{\vartheta}_2 = \beta_3 \vartheta_2$ with ϑ_2 being a positive constant. Using the Lemma 4, the third-order subsystem (14) is fixed-time stable, and s_2 will converge into a small set $\Delta_4 = \left\{ s_2 | V(s_2) \leq \min\left\{ \left(\frac{c_3}{\alpha_1 2^{\bar{p}_6}}\right)^{\frac{1}{\bar{p}_6}}, \left(\frac{c_3}{\alpha_2 2^{\bar{q}_6}}\right)^{\frac{1}{\bar{p}_6}} \right\} \right\}$ around zero in the fixed time t_{s_2}, which is determined by

$$t_{s_2} \leq \frac{1}{\alpha_4 2^{\bar{p}_6} \phi_2 (1 - \bar{p}_6)} + \frac{1}{\alpha_5 2^{\bar{q}_6} \phi_2 (\bar{q}_6 - 1)} \tag{28}$$

Then, s_2 will hold in a small region of origin, which guarantees a real sliding mode surface[23]. Therefore, the auxiliary variable ξ and its derivative $\dot{\xi}$ will also converge into the origin along the sliding mode surface[24].

Step 2 According to (25), when the auxiliary $\dot{\xi} = 0$, one has

$$\dot{x}_e = -\lambda_1 \operatorname{erf}(x_e) + \lambda_2 \operatorname{erf}(y_e) - \lambda_3 x_e y_e \operatorname{erf}(y_e) - k_1 |x_e|^{\gamma_3} \operatorname{erf}\left(\frac{x_e}{\epsilon_3}\right) \tag{29}$$

Choose a Lyapunov function as $V_5 = x_e^2$, the time derivative of V_5 is

$$\begin{aligned}\dot{V}_5 &= 2x_e\dot{x}_e \\ &= -2\Big(\lambda_1 x_e \operatorname{erf}(x_e) - \lambda_2 x_e \operatorname{erf}(y_e) + \lambda_3 x_e^2 y_e \operatorname{erf}(y_e) + k_1|x_e|^{\gamma_3}\operatorname{erf}(\frac{x_e}{\epsilon_3})\Big) \\ &\le -2\Big(\lambda_1|x_e| - \lambda_2|x_e| - \lambda_1\epsilon_4 + k_1 x_e|x_e|^{\gamma_3}\operatorname{erf}(\frac{x_e}{\epsilon_3})\Big) \\ &\le -2\Big(k_1\epsilon_3|x_e||x_e|^{\gamma_3}\operatorname{erf}(|\frac{x_e}{\epsilon_3}|) - \lambda_1\epsilon_4\Big)\end{aligned} \tag{30}$$

where ϵ_4 is a positive constant. The rest of the proof is similar to the proof of Theorem 2. There exists a constant $0 < \vartheta_3 < 1$ such that the variable x_e will reach and keep in a small region Δ_5 around the origin within a fixed time T_2:

$$T_2 \le \frac{1}{k_1\vartheta_3 e^{-\frac{\lambda_4}{2e}}} + \frac{1}{2k_1\epsilon_3(\frac{\lambda_4}{1+\mu_4} - 1)} \tag{31}$$

Then, it can be obtained that the $\dot{x}_e$ is a uniformly continuous form (29). Employ Barbalat Lemma [25] to prove $\dot{x}_e \to 0$ as $t \to \infty$, then $\dot{x}_e$ is bounded after the variable x_e converges. Hence, there exists a small region Δ_5 around the origin that y_e can converge into Δ_5.

Step 3 Before the angular error θ_e converges to zero, $\theta_e \neq 0$, such that subsystem (13) cannot be simplified as (19). It should be proved that system state variables x_e, y_e, and v are bounded before the angular error θ_e converges to zero.
Consider the following bounded function:

$$V_6 = \frac{1}{2}x_e^2 + \frac{1}{2}y_e^2 + |v| \tag{32}$$

The time derivative of V_6 is

$$\begin{aligned}\dot{V}_6 &\le |x_e||\dot{x}_e| + |y_e||\dot{y}_e| + |\dot{v}| \\ &\le |x_e||\dot{x}_e| + |y_e||\dot{y}_e| + m\Big(\omega_r\dot{y}_e + |\dot{h}(x_e, y_e)| + k_{21}\big(|\xi|^{p_4} + |\xi|^{q_4}\big) + k_{22}\big(|\dot{\xi}|^{p_5} + |\dot{\xi}|^{q_5}\big) \\ &\quad +\beta_1|s|_2^{p_6} + \beta_2|s|_2^{q_6}\Big) + \frac{|\tilde{d}_2|}{m} \\ &\le |x_e||\dot{x}_e| + |y_e||\dot{y}_e| + m\Big(|\dot{y}_e| + k_{21}\big(|\xi|^{p_4} + |\xi|^{q_4}\big) + k_{22}\big(|\dot{\xi}|^{p_5} + |\dot{\xi}|^{q_5}\big) + \beta_1|s|_2^{p_6} + \beta_2|s|_2^{q_6} \\ &\quad +\lambda_3\big(|\dot{x}_e||y_e| + |x_e||\dot{y}_e| + |x_e||y_e||\dot{y}_e|\big) + \frac{k_1\lambda_4|x_e||\dot{x}_e|}{1+\mu_0 x_e^2}|x_e|^{\gamma_3}\Big(1 + \frac{2|x_e|}{1+\mu_4 x_e^2}\Big) \\ &\quad +\frac{2k_1}{\epsilon_2\sqrt{\pi}}|x_e|^{\gamma_3}|\dot{x}_e|\Big) + \frac{|\tilde{d}_2|}{m} \\ &\le |x_e||\dot{x}_e| + |y_e||\dot{y}_e| + m\Big(|\dot{y}_e| + k_{21}\big(|\xi|^{p_4} + |\xi|^{q_4}\big) + k_{22}\big(|\dot{\xi}|^{p_5} + |\dot{\xi}|^{q_5}\big) + \beta_1|s|_2^{p_6} + \beta_2|s|_2^{q_6} \\ &\quad +\lambda_3\big(|\dot{x}_e||y_e| + |x_e||\dot{y}_e| + |x_e||y_e||\dot{y}_e|\big) + \frac{k_1\lambda_4}{\mu_4}(1 + 2|x_e|)|x_e|^{\frac{\lambda_4}{\mu_4}-1}|x_e| \\ &\quad +\frac{2k_1}{\epsilon_2\sqrt{\pi}}|x_e|^{\frac{\lambda_4}{\mu_4}}|x_e|\Big) + \frac{|\tilde{d}_2|}{m}\end{aligned} \tag{33}$$

Let $\eta_1 = \sqrt{x_e^2 + y_e^2 + |v|} \ge \eta > 1$, then one has the following inequalities: $|x_e| \le \eta_1, |y_e| \le \eta_1, |v| \le \eta_1$. Furthermore, there exist positive constants $a_i (i = 3, 4), b_l, c_l, (l = 4, 5, ..., 9)$, which satisfy $|x_e|^{\frac{\lambda_4}{\mu_4}} \le a_3\eta_1$, $|x_e|^{\frac{\lambda_4}{\mu_4}-1} \le a_4\eta_1$, $|s_2|^{p_6} < b_4 + c_4\eta_1$, $|s_2|^{q_6} < b_5 + c_5\eta_1$, $|\xi|^{p_4} < b_6 + c_6\eta_1$, $|\xi|^{q_4} < b_7 + c_7\eta_1$, $|\dot{\xi}|^{p_5} < b_8 + c_8\eta_1$,

$|\dot{\xi}|^{q_5} < b_9 + c_9\eta_1$. According to Theorem 3, the state variable θ_e, ω will converge into the origin within a fixed time t_{s_1}, then one has $\theta_e \le \theta_m$, $|\omega| \le \omega_m$, $|\tilde{d}_2| < k_d$. Further $|\dot{y}_e| < |\dot{x}_e| \le v_{1_{\max}} + \omega_m\eta_1$ can be obtained. Then, (33) can be simplified as

$$\begin{aligned}\dot{V}_6 \le\ & (2\eta_1 + 2m\lambda_3 + \eta_1^2 + m)(v_{1_{\max}} + \omega_m\eta_1) + \frac{mk_1\lambda_4}{\mu_4}(v_{1_{\max}} + \omega_m\eta_1)a_4\eta_1 \\ & + \frac{2mk_1}{\epsilon_2\sqrt{\pi}}a_3\eta_1(v_{1_{\max}} + \omega_m\eta_1) + \frac{k_d}{m} \\ \le\ & \frac{\eta_1^2}{2}2\Big(2v_{1_{\max}} + 3\omega_m + 2m\lambda_3 + m + \frac{2mk_1a_4\lambda_4}{\mu_4}(v_{1_{\max}} + \omega_m) + \frac{2ma_3k_1}{\epsilon_2\sqrt{\pi}}(v_{1_{\max}} + \omega_m)\Big) \\ & + 2m\lambda_3 v_{1_{\max}} + \frac{k_d}{m} \\ \le\ & KV_6 + \varrho_1\end{aligned} \tag{34}$$

where K and ϱ_1 satisfy the following constraints:

$$K = 2\Big(2v_{1_{\max}} + 3\omega_m + 2m\lambda_3 + m + \frac{2mk_1a_4\lambda_4}{\mu_4}(v_{1_{\max}} + \omega_m) + \frac{2ma_3k_1}{\epsilon_2\sqrt{\pi}}(v_{1_{\max}} + \omega_m)\Big) \tag{35}$$

$$\varrho_1 = 2m\lambda_3 v_{1_{\max}} + \frac{k_d}{m} \tag{36}$$

On the contrary, if $\eta_1 > 1$, there exists a positive constant ϱ_2, which satisfies $\dot{V}_6 \le \varrho_2$. One has $\dot{V}_6 \le KV_6 + \varrho_3$ for the state variable x_e, y_e, v. Further, before the angular error θ_e converges to zero, one can obtain

$$V_6 \le \big(V_6(0) + \frac{\varrho_3}{K}\big)e^{Kt} - \frac{\varrho_3}{K} \tag{37}$$

Remark 1 The auxiliary variable ξ in (24) can reduce the order of the third-order subsystem, which simplifies the process of the controller design. In addition, the controller developed in this paper can guarantee that the system state variables converge in a fixed time and the chattering problem is solved by using the error function erf(·). Furthermore, utilizing the variable exponent coefficient in (24) avoids the common singularity problem.

4. EXPERIMENT RESULTS

To verify the effectiveness of the proposed control scheme, the trajectory tracking experiment is implemented on a Quanser QBot 2e mobile robot platform composed of a QBot 2e mobile robot, an OptiTrack system with 12 infrared cameras, and a computer. The experimental platform is presented in Figure 2. The whole closed-loop experiment structure is as follows: The simulation diagram is compiled on the host computer equipped with MATLAB/Simulink to transform the simulation into an executable file. And the control scheme is written to the Gumstix computer embedded in the QBot 2e through wireless communication protocol. The real-time position information of the QBot 2e is obtained by the OptiTrack positioning system. Then the host computer calculates the information and transmits them to the embedded computer of a WMR for the input of real-time calculation of executable files. So as to complete the trajectory experiment of the mobile robot.

In the experiment, the physical parameters of the QBot 2e are chosen as follows: $m = 4$ kg, $J = 2.5$ kg $\cdot$ m^2. The desired reference trajectory is set as $x_r = \cos(0.2t)$ m, $y_r = \sin(0.2t)$ m. The initial values of the reference and practical trajectories are $[x_r(0), y_r(0), \theta_r(0)]^{\mathrm{T}} = [1, 0, \pi/2]^{\mathrm{T}}$, $[x(0), y(0), \theta(0)]^{\mathrm{T}} = [0.7, -0.02, \pi/6]^{\mathrm{T}}$, respectively. The main relevant parameters of the proposed control scheme are as follows: $k_1 = 0.001$, $k_{11} = k_{12} = 0.9$, $k_{21} = 0.05$, $k_{22} = 0.06$, $\epsilon_2 = 0.00001$. Choose the parameters $\alpha_1 = 2$, $\alpha_2 = 0.5$, $\beta_1 = \beta_2 = 1$ for the sliding mode surface s_1 in (17) and s_2 in (25), respectively.

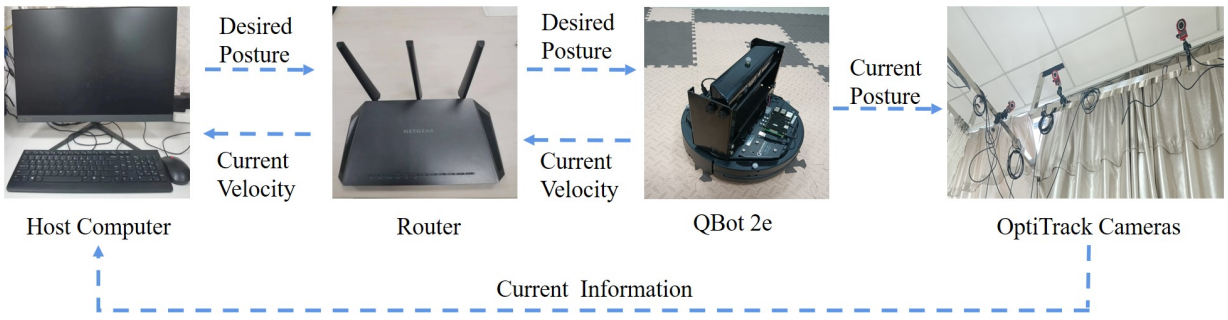

Figure 2. The Quanser QBot 2e Mobile Robot Platform.

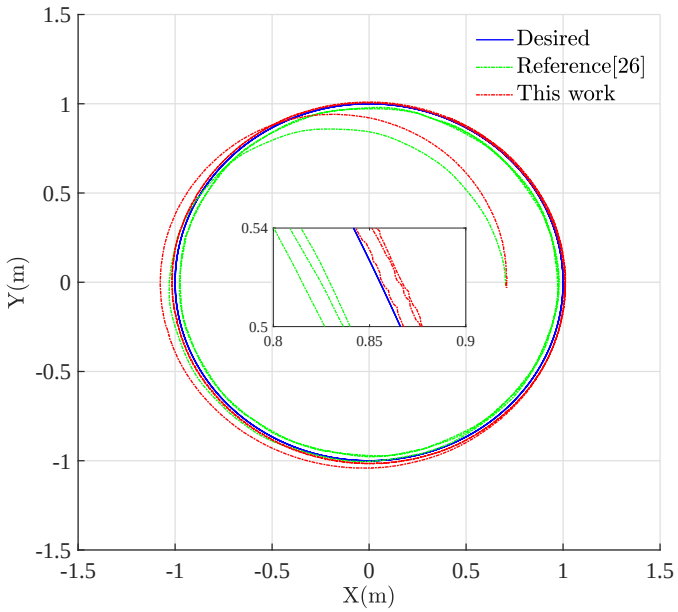

Figure 3. The comparative trajectory tracking experiment results of the WMR. WMR: wheeled mobile robot.

It is obvious that the WMR trajectory tracking mission can be achieved by the designed control method as plotted in the red track in Figure 3. The time response curves of the sliding mode surfaces, s_1 and s_2, are shown in Figure 4, which converge very quickly. To illustrate the excellence of the proposed control method, a comparative experiment on the trajectory tracking of WMRs is conducted between this work and reference [26]. The control inputs of the designed control scheme and reference are shown in Figure 5, which are nonsingular and continuous. Figure 6 illustrates the tracking errors in this experiment, which have a big fluctuation due to the influence of external disturbances. In the experiment, the external disturbance is from the experimental environment, such as uneven ground. The observed disturbance values are shown in Figure 7, which indicates the effectiveness of the proposed disturbance observer in this work. From the experimental results, it can be concluded that the designed control scheme has the robustness against the external disturbance and high tracking accuracy.

5. DISCUSSION

In this paper, a universal control scheme for fixed-time trajectory tracking based on ISMC is put forward. The dynamic model of the WMR has been transformed into two error subsystems. Then utilizing the fixed-time technology and ISMC, a new fixed-time disturbance observer has been proposed and applied on the two error subsystems. Furthermore, an observer-based tracking control method has been proposed to achieve

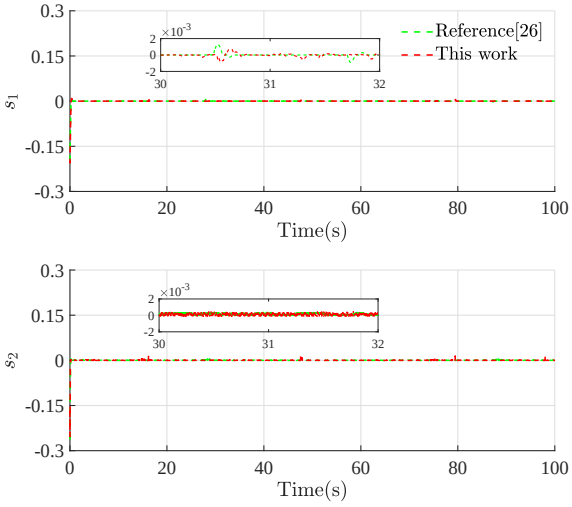

Figure 4. Comparative results of sliding mode surfaces in the experiment.

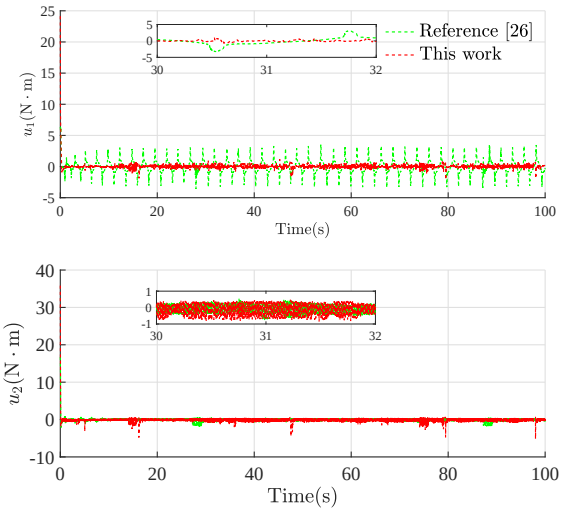

Figure 5. Comparative results of control torques in the experiment.

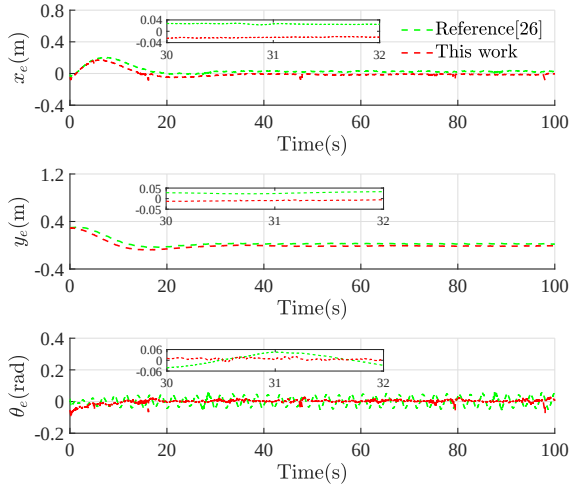

Figure 6. Comparative results of tracking errors x_e, y_e, θ_e in the experiment.

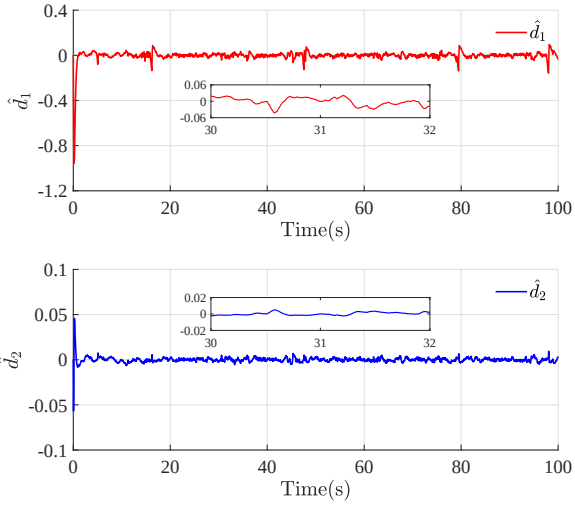

Figure 7. Disturbance estimation $\hat{d}_1$ and $\hat{d}_2$ in the experiment.

a trajectory tracking mission for the WMR, and guarantee the tracking error converges within a fixed time. Finally, the proposed control approach has been verified by a mobile robotic platform, and the experimental results show fine control performances. Our future work will focus on how to realize the formation tracking control of multi-wheeled mobile robots in both theory and experiment.

DECLARATIONS

Acknowledgments

The authors would like to thank the editors and reviewers for their valuable comments dedicated to this article.

Authors' contributions

Made significant contributions in writing, methodology, review: Li B
Executed writing-original draft, experiment verification: Ma L
Methodology validation: Wang C

Data result analysis: Ge C
Supervision and modification: Liu H

Availability of data and materials
Not applicable.

Financial support and sponsorship
This work was supported in part by the National Natural Science Foundation of China (62073212), Natural Science Foundation of Shanghai (23ZR1426600), and Innovation Fund of Chinese Universities Industry-University-Research (2021ZYB05004).

Conflicts of interest
All authors declared that there are no conflicts of interest.

Ethical approval and consent to participate
Not applicable.

Consent for publication
Not applicable.

REFERENCES

1. Panahandeh P, Alipour K, Tarvirdizadeh B, Hadi A. A kinematic Lyapunov-based controller to posture stabilization of wheeled mobile robots. *Mech Syst Signal Pr* 2019;134:1–19. DOI
2. Huang H, Li Y, Bai Q. An improved a star algorithm for wheeled robots path planning with jump points search and pruning method. *Complex Eng Syst* 2022;2:11. DOI
3. Kanayama Y, Kimura Y, Miyazaki F, Noguchi T. A stable tracking control method for an autonomous mobile robot. In: Proceedings., IEEE International Conference on Robotics and Automation; 1990;1. pp. 384–89. DOI
4. Fierro R, Lewis F. Control of a nonholonomic mobile robot: backstepping kinematics into dynamics. In: Proceedings of 1995 34th IEEE Conference on Decision and Control; 1995;4. pp. 3805–10. DOI
5. Bloch A. Nonholonomic mechanics and control. Interdisciplinary Applied Mathematics. New York, NY: Springer; 2003. DOI
6. Murray R, Sastry S. Nonholonomic motion planning: steering using sinusoids. *IEEE Trans Automat Contr* 1993;38:700–16. DOI
7. Tayebi A, Tadjine M, Rachid A. Invariant manifold approach for the stabilization of nonholonomic chained systems: Application to a mobile robot. *Nonlinear Dynam* 2001;24:167–81. DOI
8. Wang X, Zhang G, Neri F, et al. Design and implementation of membrane controllers for trajectory tracking of nonholonomic wheeled mobile robots. *Integr Comput-Aid E* 2016;23:15–30. DOI
9. Zhai J, Song Z. Adaptive sliding mode trajectory tracking control for wheeled mobile robots. *Int J Control* 2019;92:2255–62. DOI
10. Ou M, Sun H, Zhang Z, Li L. Fixed-time trajectory tracking control for multiple nonholonomic mobile robots. *T I Meas Control* 2021;43:1596–608. DOI
11. Li B, Zhang H, Xiao B, Wang C, Yang Y. Fixed-time integral sliding mode control of a high-order nonlinear system. *Nonlinear Dynam* 2022;107:909–20. DOI
12. Liu Q, Cai Z, Chen J, Jiang B. Observer-based integral sliding mode control of nonlinear systems with application to single-link flexible joint robotics. *Complex Eng Syst* 2021;1:8. DOI
13. Zhang Z, Leibold M, Wollherr D. Integral sliding-mode observer-based disturbance estimation for euler–lagrangian systems. *IEEE Trans Contr Syst T* 2020;28:2377–89. DOI
14. Li B, Hu Q, Yang Y. Continuous finite-time extended state observer based fault tolerant control for attitude stabilization. *Aerosp Sci Technol* 2019;84:204–13. DOI
15. Zhang H, Li B, Xiao B, Yang Y, Ling J. Nonsingular recursive-structure sliding mode control for high-order nonlinear systems and an application in a wheeled mobile robot. *ISA T* 2022;130:553–64. DOI
16. Chevillard S. The functions erf and erfc computed with arbitrary precision and explicit error bounds. *Inform Comput* 2012;216:72–95. DOI
17. Eltayeb A, Rahmat M, Basri MAM, Mahmoud MS. An improved design of integral sliding mode controller for chattering attenuation and trajectory tracking of the quadrotor UAV. *Arab J Sci Eng* 2020;45:6949–61. DOI

18. Ba D, Li Y, Tong S. Fixed-time adaptive neural tracking control for a class of uncertain nonstrict nonlinear systems. *Neurocomputing* 2019;363:273–80. DOI
19. Bagul Y, Chesneau C. Sigmoid functions for the smooth approximation to the absolute value function. *MJPAA* 2021;7:12–19. DOI
20. Polycarpou M, Ioannou P. A robust adaptive nonlinear control design. *Automatica* 1996;32:423–27. DOI
21. Jiang Z, Nijmeijer H. Tracking control of mobile robots: A case study in backstepping. *Automatica* 1997;33:1393–99. DOI
22. Wang C, Wen G, Peng Z, Zhang X. Integral sliding-mode fixed-time consensus tracking for second-order non-linear and time delay multi-agent systems. *J Franklin I* 2019;356:3692–710. DOI
23. Plestan F, Shtessel Y, Brégeault V, Poznyak A. New methodologies for adaptive sliding mode control. *Int J Control* 2010;83:1907–19. DOI
24. Song T, Fang L, Wang H. Model-free finite-time terminal sliding mode control with a novel adaptive sliding mode observer of uncertain robot systems. *Asian J of Control* 2022;24:1437–51. DOI
25. Li B, Gong W, Yang Y, Xiao B, Ran D. Appointed fixed time observer-based sliding mode control for a quadrotor UAV under external disturbances. *IEEE Trans Aero Elec Sys* 2022;58:290–303. DOI
26. Tian B, Liu L, Lu H, et al. Multivariable finite time attitude control for quadrotor UAV: Theory and experimentation. *IEEE Trans Ind Electron* 2018;65:2567–77. DOI